EXPERIMENTAL STUDY TO DETERMINE THE TENSION SOFTENING CURVE OF CONCRETE

(Translation from the Journal of Materials, Concrete Structures and Pavements, JSCE, No.606/V-41, November 1998)

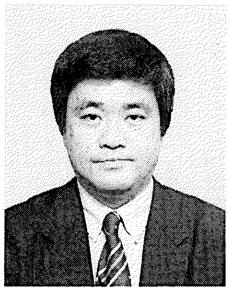
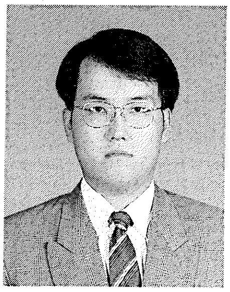
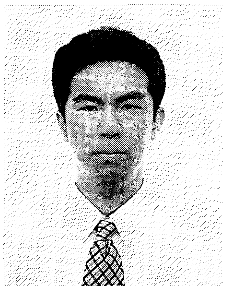

Junichiro NIWA   Taweechai SUMRANWANICH   Toyofumi MATSUO

A new method of determining the tension softening curve of concrete is proposed in this study. To overcome the problems associated with the modified J-integral method, the release of elastic energy is quantitatively evaluated, through the unloading and reloading of notched beams subjected to a concentrated load. In addition, based on measurements of the distribution of fictitious crack width within the ligament portion of a notched beam, the propagation of fictitious cracks has been evaluated quantitatively. The new method, in which these new findings are incorporated, is used to estimate the tension softening curves of various types of concrete at various ages, and the validity of the method is confirmed experimentally by comparing the tension softening curves with each other.

Key words: *tension softening curve, fracture mechanics, J-integral method, fictitious crack, elastic energy*

Junichiro NIWA is a Professor of the Department of Civil Engineering at Tokyo Institute of Technology, Tokyo, Japan. He received his Doctor of Engineering Degree from the University of Tokyo in 1983. He has served as Secretary General of the Concrete Committee of the JSCE from April 1999. He specializes in the mechanics of structural concrete including fracture mechanics, shear problems, and the application of FEM analysis. He is a member of the JSCE, JCI, ACI, IABSE, and fib.

Taweechai SUMRANWANICH is a Lecturer in the Department of Civil Engineering at Burapha University, Chonburi, Thailand. He received his Master of Engineering Degree from Asian Institute of Technology, Bangkok, Thailand in 1997. His research interests are related to improving methods of determining the tension softening diagram of concrete based on experimental and analytical examinations. He is a member of EIT.

Toyofumi MATSUO is a researcher of the Structural Division at the Central Research Institute of the Electric Power Industry, Chiba, Japan. He received his Master of Engineering Degree from Nagoya University, Nagoya, Japan in 1995. His research interests are related to the fracture mechanics of concrete and structural concrete and the application of nonlinear FEM analysis. He is a member of the JSCE and JCI.

1. INTRODUCTION

The tension softening characteristic of concrete, along with its fracture energy, is an important parameter in determining the fracture property of the concrete. The fracture property of a concrete structure can be quantitatively analyzed only when both the tension softening characteristic and fracture energy have been clarified. Further, the tension softening characteristic provides information important in evaluating the fracture property of various types of concrete, especially for their strength evaluation. As this makes clear, the tension softening characteristic of concrete is an important one. However, to date, no standard test method has been established for its determination. Although RILEM's three-point notched beam bending test is considered the standard method for evaluation of fracture energy, no such standard for evaluating the tension softening curve has been established.

Methods currently in use for determining the tension softening curve are divided into two groups: (1) numerical analysis methods based on inverse analysis and (2) J-integral methods based on the energy balance. Typical of the former is a method in which the relationship between load and displacement is measured and a fictitious crack model analysis is carried out; then the tension softening curves are individually calculated so the results coincide with the measurements obtained [1], [2]. With this type of method, tension softening curves are obtained sequentially such that they coincide with test results; this makes the method widely applicable. It is a smart and powerful method. However, in order to standardize a test method, it is necessary to prepare a simple-to-use program for analysis. This approach has in fact been tried [3], and further developments are expected in future.

In contrast, the inverse analysis method is applicable regardless of whether the phenomenon of crack propagation in concrete is understood. This is one advantage of the inverse analysis method, but it also leads to no findings related to crack propagation, so it makes no contribution to clarification of the actual phenomenon. On the other hand, starting with the J-integral based method by Li, et al.[4], a series of methods based on energy balance have been proposed: the new J-integral based method [5], and the modified J-integral based method [6]. Although it has been pointed out that these methods suffer from problems relating to the accuracy of measured data and the propriety of the assumptions used, they can, unlike the inverse analysis method, help improve understanding of the fracture phenomenon and, therefore, improve the accuracy of estimation of the tension softening curve.

In this study, the release of elastic energy when energy is consumed and the propagation of fictitious cracks in the ligament portion are highlighted and evaluated to propose an accurate method of determining the tension softening curve.

2. CONVENTIONAL METHODS OF DETERMINING TENSION SOFTENING CURVE

2.1 Outline of Methods Based on Energy Balance

Figure 1 shows an example of a tension softening curve. Here, σ is the softening stress and ω is the width of a fictitious crack. The reason why the fictitious crack is strengthened here is to clearly indicate that this is not the actual crack width but is obtained through the integration of displacement accompanying the development of micro cracks.

When the energy consumed per unit area of fictitious cracks up until the width of the fictitious crack reaches ω is $e(\omega)$, the following equation is obtained:

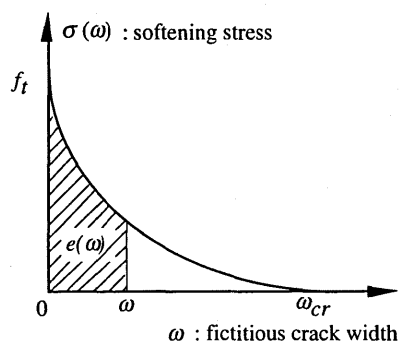

Figure 1. Example of Tension Softening Curve

$$e(\omega) = \int_0^{\omega} \sigma(\omega)\, d\omega \tag{1}$$

When the softening stress falls to zero, the corresponding width of the fictitious crack is ω_{cr}. The following equation is obtained from the definition:

$$e(\omega_{cr}) = \int_0^{\omega_{cr}} \sigma(\omega)\, d\omega = G_F \tag{2}$$

Where, G_F is the fracture energy of concrete. From Eq. (1), if the consumed energy $e(\omega)$ is obtained, the softening stress can be calculated as follows:

$$\sigma(\omega) = \frac{d}{d\omega} e(\omega) \tag{3}$$

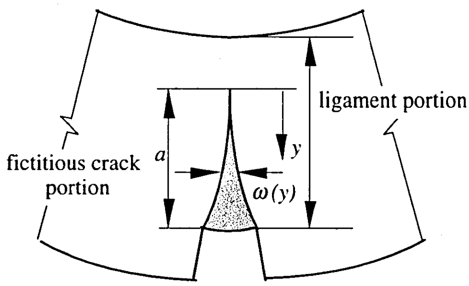

Figure 2. Distribution of Fictitious Crack Width on Beam

As illustrated in Figure 2, in the ligament portion of a beam with a width of b, the energy E consumed until the length of the fictitious crack reaches a is calculated by the following equation:

$$E = b \int_0^{a} e(\omega(y))\, dy \tag{4}$$

In Eq. (4), $\omega(y)$ is the fictitious crack width at position y. If the consumed energy E calculated from Eq. (4) is provided in the form of external work, the fictitious crack will propagate.

If E, a, and $\omega(y)$ are experimentally determined, $e(\omega)$, and subsequently $\sigma(\omega)$ can be determined using Eq. (3). This is an outline of the method of the energy-balance method of determining the tension softening curve.

2.2 J-Integral Method by Li, et al.

In the J-integral method described by Li, et al.[4], two specimens are prepared, exactly the same in all respects except for slightly different initial ligament depths, and load-deflection curves for the specimens are measured; the difference between the curves is assumed to result from the difference in crack height of the specimens and the relationship between the width ω of the fictitious crack and the consumed energy $e(\omega)$ is calculated.

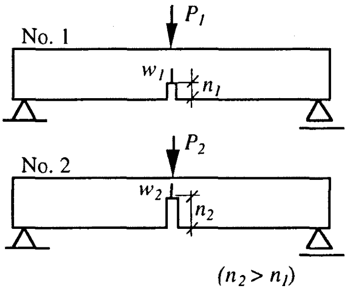

Figure 3. Two Specimens with Different Ligament Depths

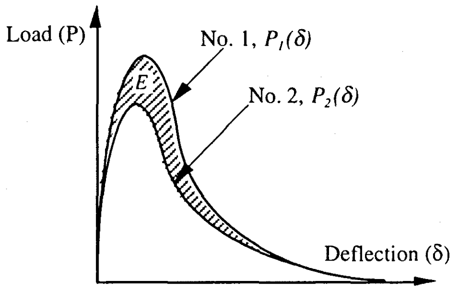

Figure 4. Relationship between Load and Deflection for Two Specimens

In other words, bending tests are performed on two specimens identical except for their initial ligament depths, as shown in Figure 3, and when results such as those shown in Figure 4 are obtained, all differences in the curves shown in Figure 4 are assumed to result from the difference a in the ligaments and $e(\omega)$ is calculated using Eq. (5).

$$e(\omega) = E(\omega) / (b \cdot a) \tag{5}$$

$$a = n_2 - n_1$$

$$\omega = \omega(\delta) = \frac{w_1(\delta) + w_2(\delta)}{2}$$

$$E(\omega) = E(\omega(\delta)) = \int_0^{\delta} \{P_1(\delta) - P_2(\delta)\}\, d\delta$$

where, n_1 and n_2 are the notch depths of the respective beams and $n_1 < n_2$; and ω is the width of the fictitious crack at the point of deflection δ and is assumed to be the average of crack mouth openings w_1 and w_2 which are measured for both beams. Further, the distribution of fictitious crack width $\omega(y)$ in the depth difference a of the ligament portions is assumed to be uniform. From the above assumptions, the relationship shown in Eq. (5) is obtained.

In the J-integral method by Li, et al., no special test equipment is required. The notched beam bending test is simply carried out in accordance with the RILEM Standard to measure the relationships between load and deflection, and load and crack mouth opening. Although this method is logical, two specimens are required; even though the two specimens are exactly the same. The sensitivity of the test often results in fluctuations in measured values. This is considered a weak point of the J-integral method.

2.3 New J-Integral Method by Rokugo, et al.

One problem with Li's J-integral method by Li, is that the two specimens are assumed to be exactly the same. To overcome this shortcoming, Rokugo, et al.[5] proposed a new simplified J-integral method, in which an imaginary specimen whose notch reaches the upper edge (that is, without a ligament portion) is considered as a substitute for the deeper-notched specimen in the standard J-integral method. Thus, only one specimen of ligament depth a_o is actually used to measure the relationship between load and deflection, and load and crack mouth opening.

With the above method, the difference a in ligament depth in the J-integral method is identical to the ligament depth a_o of the actual specimen. In addition, since the crack mouth opening in the imaginary specimen is zero, the fictitious crack width ω is one-half of the crack mouth opening w in the actual specimen ($\omega = w/2$). In this new J-integral method, as in Li's method, it is assumed that the

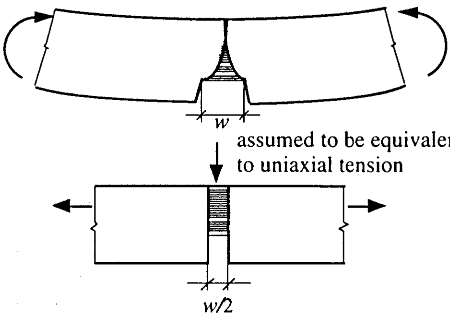

Figure 5. Assumption of Uniaxial Tension in New J-Integral Based Method

distribution of fictitious crack width is uniform within $a = a_o$, which means that, as shown in Figure 5, the behavior of a ligament portion subjected to bending is assumed to be equivalent to its behavior under uniaxial tension.

Externally applied energy can be calculated from the area below the load-deflection curve. In practice, the effect of the specimen's self weight must also be considered. When this energy is assumed to be consumed in the ligament portion, the following relationship is obtained:

$$E(\omega) = A_{lig} \cdot e(\omega) \tag{6}$$

where, $A_{lig} = b\, a_o$ = the area of the ligament portion. Further, the energy applied up until the crack mouth opening becomes w is calculated as follows:

$$E(\omega) = \int_0^{\delta_w} P(\delta)\, d\delta \tag{7}$$

where, δ_w is the deflection when the crack mouth opening becomes w. From Eqs. (6) and (7), $e(\omega)$ is obtained as follows:

$$e(\omega) = \frac{1}{A_{lig}} \int_0^{\delta_w} P(\delta)\, d\delta \tag{8}$$

This new J-integral method is both practical and simple. It does require some assumptions, which result in somewhat lower accuracy of calculation. However, the new J-integral method is superior to the original one in that it is not significantly affected by the fluctuations in test data. It proves useful for rough evaluation of the tension softening curve and in cases the tension softening curves of several types of concrete are compared against each other.

The method does, however, make the assumption that the fictitious crack propagates throughout the ligament portion immediately after loading; that the energy released after accumulation in the elastic region can be ignored; that the distribution of fictitious crack width is uniform in a_o; and that the width is one-half of the crack mouth opening. These assumptions do not accurately reflect the actual phenomena, so there is room for improvement.

2.4 Modified J-Integral Method by Uchida, et al.

In place of the above new J-integral method, Uchida, et al. proposed a modified J-integral method [6]. Uchida, et al. point out three problems that they attempt to solve:

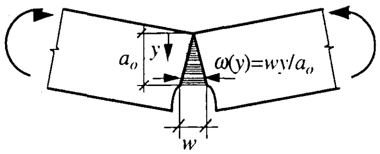

Figure 6. Fictitious Crack Distribution in the Modified J-Integral Method

a) the assumption that the fictitious crack width ω is one-half of the crack mouth opening w, and that the fictitious crack width is uniformly distributed in the ligament portion;
b) the assumption that energy applied to a specimen is completely consumed in the fictitious crack portion; and
c) the assumption that the fictitious crack propagates throughout the ligament portion immediately after loading.

In their modified J-integral method, assumption (a) is modified. In other words, the fictitious crack is not uniformly distributed, but (as shown in Figure 6) the crack is assumed to be distributed as if it was rotating around an axis located at the compression fiber on the upper portion of the notch.

Therefore, the fictitious crack width is calculated as follows.

$$\omega(y) = w\, y / a_o \tag{9}$$

As a result, the energy consumed in the fictitious crack region is obtained as follows:

$$E = b\int_0^a e(\omega(y))\, dy = b\int_0^w e(\omega)\frac{a_o}{w}\, d\omega$$
$$= \frac{A_{lig}}{w}\int_0^w e(\omega)\, d\omega \tag{10}$$

Equation (10) is differentiated by w to obtain the following relationship:

$$e(w) = \frac{1}{A_{lig}}\left[E(w) + w\frac{dE(w)}{dw}\right] \tag{11}$$

Equation (11) is further differentiated by w to obtain the following relationship:

$$\sigma(w) = \frac{de(w)}{dw} = \frac{1}{A_{lig}}\left[2\frac{dE(w)}{dw} + w\frac{d^2E(w)}{dw^2}\right] \tag{12}$$

$E(w)$ is obtained in the same manner as for Eq. (7). Replacement of w in Eq. (12) with ω provides the tension softening curve; however, the effect of the specimen's self weight must also be considered.

As described above, the assumption of fictitious crack width in the modified J-integral method is more realistic than the uniform distribution of the new J-integral method. As a result, the modified J-integral method is judged to more accurately estimate the tension softening curve.

3. PROBLEMS WITH CONVENTIONAL EVALUATION METHODS

3.1 Outline

The modified J-integral method uses a modified fictitious crack width distribution, thus overcoming

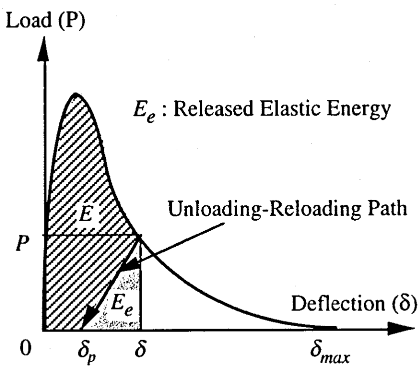

Figure 7. Release of Elastic Energy in Load-Deflection Diagram

one of the problems of the earlier method. However, the assumptions that externally applied energy is completely consumed in the fictitious crack portion and that the fictitious crack propagates throughout the ligament portion immediately after loading remain. It is thought that if these assumptions were brought closer to reality, the tension softening curve could be more accurately evaluated. Therefore, it is these two assumptions that are dealt with in this study.

3.2 Release of Elastic Energy

In both the new and modified J-integral methods, the externally supplied energy is calculated using Eq. (7). Actually, this is a potential energy, though it is assumed to be consumed completely in the fictitious crack portion for convenience. However, part of the energy actually accumulates in zones other than the fictitious crack, and this energy must be released as elastic energy at unloading, as shown in Figure 7. Therefore, in order to properly evaluate the energy consumed in the fictitious crack portion, the amount of elastic energy released must be deducted from the total potential energy.

To do this, the unloading-reloading path in the softening region of the load-deflection curve has to be clarified. In this study, the unloading-reloading path was clarified through experiment, and based on this, the released elastic energy was quantitatively evaluated.

The dark colored portion in Figure 7 is the released elastic energy E_e; that is, it represents the energy not consumed in the fictitious crack portion. Therefore, if the unloading-reloading path can be determined, the consumed energy E can be obtained. For example, if the unloading-reloading path is determined to be linear, E is estimated using Eq. (13).

$$E(w) = \int_0^{\delta} P(\delta)\, d\delta - \frac{1}{2} P(\delta)\left(\delta - \delta_p\right) \tag{13}$$

In Eq. (13), δ_p is the residual deflection in a fully unloaded state. To account for the effect of the specimen's self weight, one-half of the self weight of the specimen is added to $P(\delta)$.

3.3 Evaluation of Propagation of Fictitious Crack

Immediate propagation of the fictitious crack throughout the ligament portion immediately after loading is simply an assumption. Actually, it must gradually propagate as the deflection increases. As indicated in Figure 8, when the ligament depth is a_o, the fictitious crack length is a and the fictitious crack width is $\omega(y)$, the following relationships are realized:

$$\begin{aligned} \omega(y) &= \frac{y}{a} w \\ y &= \frac{a}{w} \omega(y) \\ dy &= \frac{a}{w} d\omega \end{aligned} \tag{14}$$

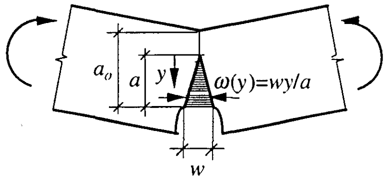

Figure 8. Fictitious Crack Propagation in Ligament Portion

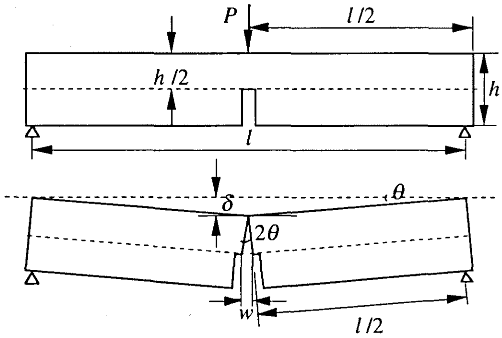

Figure 9. Rigidly Deformed State of Notched Beam

Then, the energy E consumed in this portion is calculated as follows:

$$E = b\int_0^w e(\omega)\,\frac{a}{w}\,d\omega = \frac{b\,a}{w}\int_0^w e(\omega)\,d\omega \tag{15}$$

From Eqs. (13) and (15),

$$\frac{b\,a}{w}\int_0^w e(\omega)\,d\omega = \int_0^\delta P(\delta)\,d\delta - \frac{1}{2}P(\delta)\left(\delta - \delta_p\right) = E(w)$$

$$\int_0^w e(\omega)\,d\omega = \frac{w}{b\,a}E(w)$$

$$e(w) = \frac{1}{b\,a}\left[E(w) + w\frac{dE(w)}{dw}\right]$$

$$\sigma(w) = \frac{de(w)}{dw} = \frac{1}{b\,a}\left[2\frac{dE(w)}{dw} + w\frac{d^2E(w)}{dw^2}\right] \tag{16}$$

3.4 Consideration of Propagation of Fictitious Crack

In order to evaluate whether in fact the fictitious crack propagates immediately after loading, the following examination was conducted. We assumed the deformation of a beam with a notch extending to one-half of the height, as shown in Figure 9. In this figure, the deformation at the fictitious crack takes precedence, and other portions are assumed to undergo rigid deformation. When the fictitious crack propagates throughout the ligament portion, the following relationships must be upheld between the deflection in the specimen δ, the crack mouth opening w, the span l, and the height h with deflection angle θ:

$$\delta = l\theta / 2 \tag{17}$$

$$w = (h/2)2\theta = h\theta \tag{18}$$

From Eqs. (17) and (18), the following relationship is obtained:

$$\frac{\delta}{w} = \frac{l}{2h} \tag{19}$$

In the notched beam bending test recommended by RILEM, l = 80 cm and h = 10 cm; therefore, δ/w = 4.0. As a result, if the relationship between δ and w is linear and the ratio is 4.0, it is reasonable to assume that the fictitious crack propagates throughout the ligament portion immediately after loading. However, if this is not the case, a more appropriate assumption for the propagation of the fictitious crack is required.

4. TEST PROCEDURE

4.1 Purpose of Test

In order to obtain information on the release of elastic energy and the propagation of the fictitious crack, we decided to conduct a notched beam bending test according to the RILEM recommendation. To determine the unloading-reloading path in the softening region, we carried out repeated loading in the softening region. Further, five π-type displacement gages were fitted in the ligament portion to measure the strain in that portion and clarify the propagation of the fictitious crack.

4.2 Materials Used

Ordinary Portland cement (specific gravity of 3.15) was used. Fly ash (of specific gravity 2.27, corresponding to ASTM C-type) and silica fume (specific gravity = 2.20) were mixed with the cement. River sand (specific gravity = 2.60, FM = 2.85, water absorption ratio = 1.17%) was used as the fine aggregate, and crushed limestone (specific gravity = 2.66, water absorption ratio = 0.72%) was used as the coarse aggregate (max. diameter = 16 mm); a naphthalene-type super plasticizer was used.

In the test program, three types of concrete were produced as shown in Table 1. The slump flow of the self-compacting concrete averaged 61 cm, while the slump values for the high-strength and ordinary-strength concretes were 1.5 cm and 7.5 cm, respectively.

Table 1. Mixing Proportion of Concrete

Type of Concrete	W/B (%)*	s/a (%)	Unit Weight (kg/m^3)							
			W	C	F.A.	S.F.	S	G	S.P. (%)*	Air (%)
Self-Compacting	24	58	159	530	133	—	896	664	2.2	2.0
High-Strength	22	42	116	488	—	37	768	1084	2.4	1.0
Normal-Strength	60	45	190	316	—	—	819	1024	—	1.0

* W/B is the ratio by weight of water and combining materials, such as cement + fly ash or cement + silica fume.
** Amount of S.P. is the ratio by weight to combining materials.

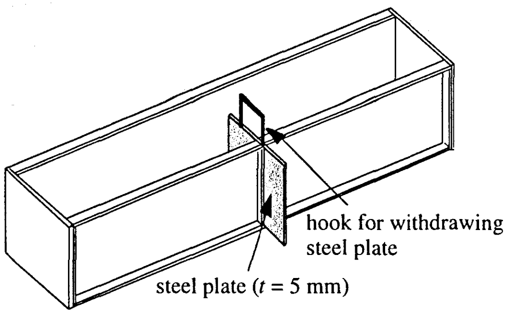

Figure 10. Steel Mold for Notched Beam

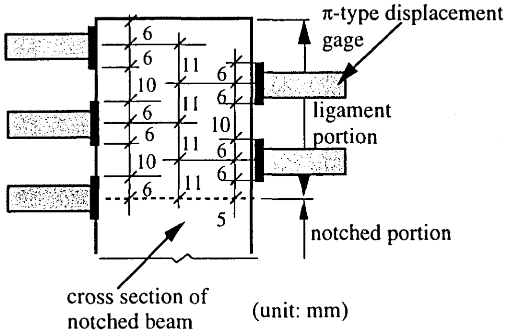

Figure 11. Allocation of π-Type Displacement Gages

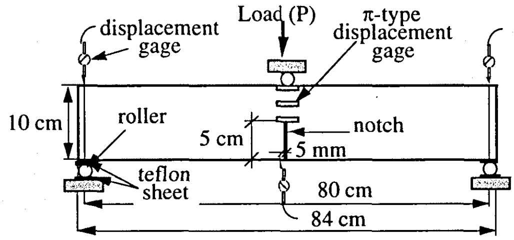

Figure 12. Loading and Measurement Conditions of Notched Beam

4.3 Specimen

The notched beams used in the experiment had a 10 cm × 10 cm cross section and 84-cm long. Twelve such specimens were prepared for each type of concrete to permit testing of three specimens at 1 day, 3 days, 7 days and 28 days. As shown in Figure 10, a 5-mm thick steel plate was inserted into the specimen before casting; the plate was withdrawn before hardening to form the notch.

After casting, the concrete was maintained in a wet condition to prevent drying, and except for specimens to be tested at 1 day, all specimens were cured in water immediately after removal from the molds. In addition to notched beam specimens, cylindrical specimens (ϕ 10 × 20 cm) were prepared as control specimens for strength. A total of 24 cylindrical specimens were prepared for each type of concrete: three for compression tests and three for splitting tests at each age.

For the experiment, the surface of the notched beam was smoothed using sand paper as bases for π-type displacement gages (distance between marks = 100 mm, width = 12 mm). These gages were bonded to the specimen using these bases (Figure 11). For the purpose of obtaining as much measurement data as possible toward clarifying the state of fictitious crack propagation, five π-type displacement gages (three on one side, two on the other side) were placed on the 5-cm high ligament portion. The five π-type displacement gages were set 11 mm apart, as shown in Figure 11.

4.4 Loading and Measurement Methods

Figure 12 shows the conditions under which the notched beams were loaded and measured. In order to prevent transverse restriction at the support, a teflon sheet was placed over and below a roller, and silicon grease was spread on the surface of the teflon sheet. A displacement-control test machine was used for loading. Displacements were measured at the supports and the center of the span and the horizontal displacement at ligament portions was measured using the five π-type displacement gages.

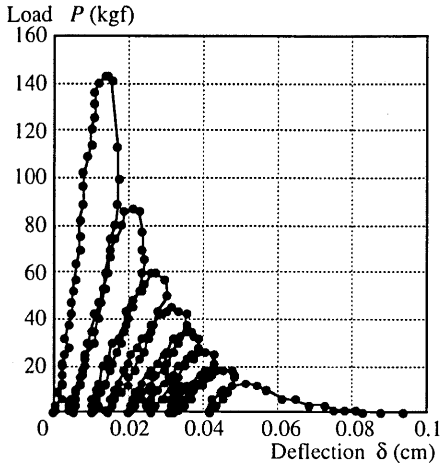

Figure 13. Example of Measured Load and Deflection for Repeated Load (self-compacting concrete at 28 days)

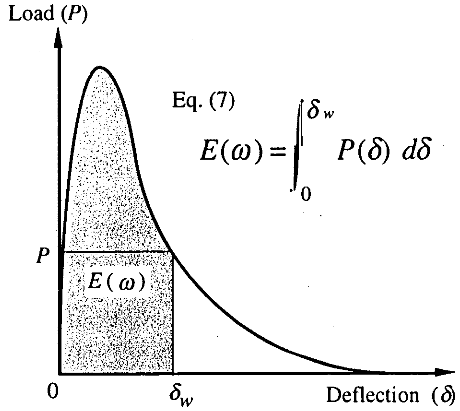

Figure 14. Meaning of "Energy" in Eq. (7)

In order to clarify the amount of elastic energy released, it was necessary to carry out unloading and reloading in the softening region, so repeated loading was carried out in the softening region. An example of the results, for self-compacting concrete at 28 days, is shown in Figure 13.

5. NEW METHOD OF DETERMINING TENSION SOFTENING CURVE

5.1 Deduction of Elastic Energy

As shown in Figure 14, the area below the load-deflection curve obtained by Eq. (7) is the potential energy, most of which is consumed in the fictitious crack portion; however, some is elastic energy released by unloading. In consideration of the balance of energy, Eq. (13) rather than Eq. (7) should therefore be used to calculate the energy consumed.

In order to determine δ_p in Eq. (13), the three types of concrete shown in Table 1 were used to conduct unloading and reloading tests in the softening region. The maximum deflection (= ultimate deflection) on the load-deflection curve is δ_{max}, the deflection when unloading starts is δ, and the residual deflection in the fully unloaded condition is δ_p; δ and δ_p are normalized by δ_{max} for all test data, and the relationships between δ_p/δ_{max} and δ/δ_{max} are plotted in Figure 15.

All test data in Figure 15 are processed in the same manner regardless of type, age, strength, or fracture energy of concrete. If the relationship between δ_p/δ_{max} and δ/δ_{max} is formulated, the portion of elastic energy released can be evaluated quantitatively. In this study, it was decided to indicate δ_p/δ_{max} simply as an exponent of δ/δ_{max}, and the exponent is determined using the method of least squares,

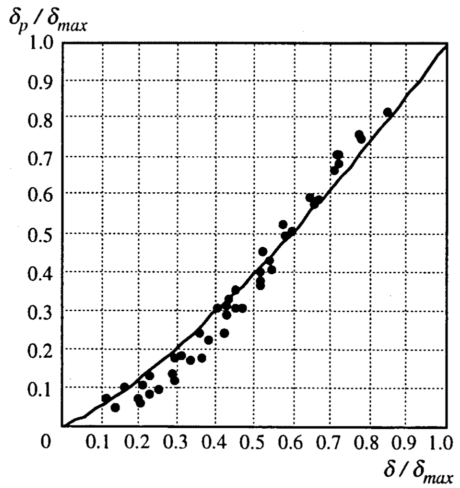

Figure 15. Relationship between δ_p/δ_{max} and δ/δ_{max}

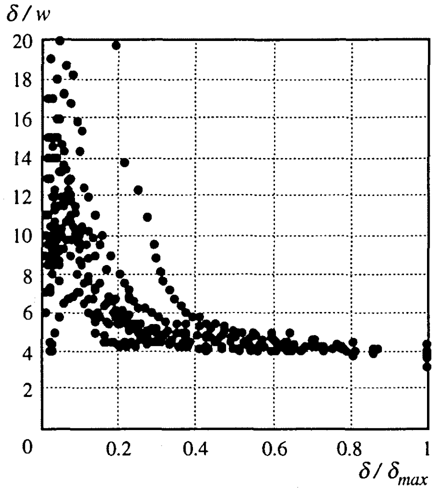

Figure 16. Relationship between δ/w and δ/δ_{max}

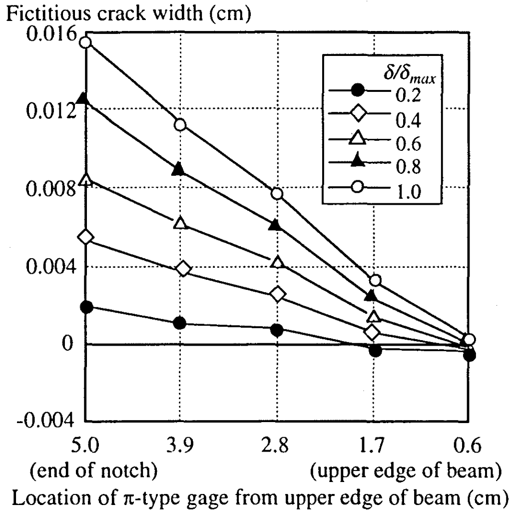

Figure 17. Propagation of Fictitious Crack (self-compacting concrete at 28 days)

shown in Figure 15 as a solid curve. This relationship is represented by Eq. (20).

$$\frac{\delta_p}{\delta_{max}} = \left(\frac{\delta}{\delta_{max}}\right)^{1.38} \tag{20}$$

Equation (20) is a simple approximation for all test data using an exponential function, and its accuracy may be open to question. Another function might have improved accuracy, but the aim of Eq. (20) is to formulate all test data and it can be considered sufficient as a first approximation. Once δ_p is determined by Eq. (20), the portion of elastic energy released can be evaluated in accordance with Eq. (13).

5.2 Relationship between Deflection of Notched Beam and Crack Mouth Opening

In order to confirm the appropriateness of the assumption that the fictitious crack propagates throughout the ligament portion from the initial stage after loading, the ratio of deflection of the notched beam to crack mouth opening δ/w was plotted against δ/δ_{max} for the three types of concrete shown in Table 1; the result is shown in Figure 16. According to the consideration in 3.4, if δ/w = 4.0, this assumption of fictitious crack propagation is appropriate.

As indicated in Figure 16, δ/w gradually approaches 4.0 as δ/δ_{max} increases. Although in the initial stage after loading, when δ/δ_{max} is small, δ/w fluctuates considerably, the value is mostly greater than 4.0, and it is recognized that the crack mouth opening is small in comparison to deflection. Therefore, the assumption that the fictitious crack propagates throughout the ligament portion immediately after loading is not appropriate. It cannot be considered appropriate to say that deformation of the notched beam resembles rigid deformation in the initial stage after loading when the deflection is small, and this is judged to be one of the factors leading to reduced accuracy of the tension softening curve.

5.3 Propagation of Fictitious Crack

The outputs from the five π-type displacement gages are assumed to be the fictitious crack widths, and their distribution is plotted in Figure 17. This example is for self-compacting concrete at 28 days. The interval between marks on the π-type displacement gages is 100 mm, and strictly speaking, the data collected from the π-type displacement gages includes the fictitious crack width, which is the accumulated value of minute deformations at micro cracks, as well as the elastic deformation in this

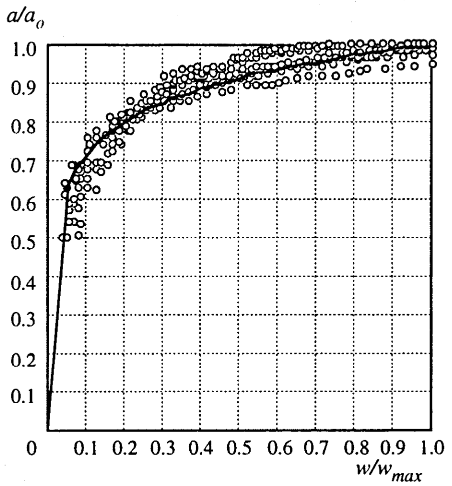

Figure 18. Relationship between Propagation of Fictitious Crack and Relative Crack Mouth Opening

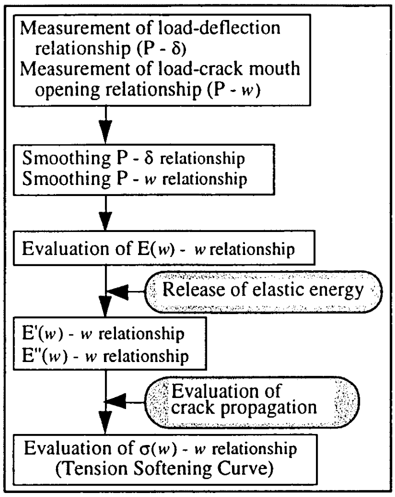

Figure 19. Proposed Method of Determining Tension Softening Curve

portion. However, the elastic stress generated here is at greatest equivalent to the tensile strength of the concrete; the resultant deformation works out to be below about 0.001 cm, which is judged negligible in comparison with the fictitious crack width. Thus, we can assume that the measured data corresponds to the fictitious crack width.

As shown in Figure 17, a clear compression zone is recognized at the upper edge of the beam at the initial stage of loading when δ/δ_{max} is 0.2 or 0.4, and it is confirmed that no fictitious crack reaches this zone. However, the compression zone narrows as deflection increases, and when δ/δ_{max} becomes 0.8, it is confirmed that the measured deformation becomes completely tensile, and the fictitious crack propagates through the upper area of the ligament portion.

If the state of fictitious crack propagation were to be indicated as a function of, for example, relative deflection δ/δ_{max} or relative crack mouth opening w/w_{max}, it would become possible to quantitatively deal with fictitious crack propagation. In Figure 18, the relative position of fictitious crack propagation a/a_o, obtained by dividing the end point a of the fictitious crack (the point at which the fictitious crack width is zero) as shown in Figure 17, by the depth a_o of the ligament portion, is plotted against w/w_{max}.

As shown in Figure 18, while the crack mouth opening is small at the initial stage of loading, the fictitious crack stops at between 50% and 80% of the ligament depth. On the other hand, as loading progresses, the end of the fictitious crack propagates to the upper edge of the beam, and when w/w_{max} becomes about 50%, a/a_o rises to 90% or more.

The solid curve in Figure 18, is derived from plotted data and calculated using Eqs. (21) and (22).

$$0.05 \leq w/w_{max} \leq 1.0 \qquad \frac{a}{a_o} = 1.0 + 0.125\, ln\left(\frac{w}{w_{max}}\right) \tag{21}$$

$$0 \leq w/w_{max} < 0.05 \qquad \frac{a}{a_o} = 12.51\frac{w}{w_{max}} \tag{22}$$

5.4 Method of Determining Tension Softening Curve

A proposed new method of determining the tension softening curve is described in Figure 19. The dark colored portion of the figure indicates the difference between the modified J-integral method and

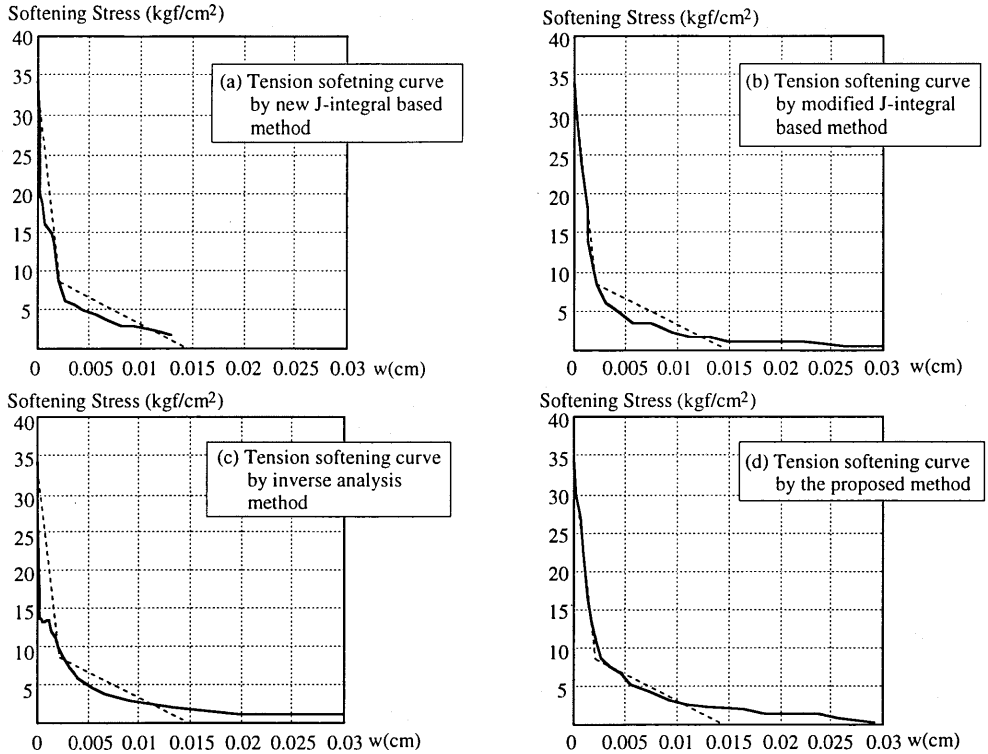

Figure 20. Tension Softening Curves for Self-Compacting Concrete (Age = 1 Day)

this new method. Based on Eq. (20), the release of elastic energy is taken into account, and from Eqs. (21) and (22), the propagation of fictitious crack in the ligament portion is evaluated. These two points are the newly introduced steps in the proposed method of determining the tension softening curve.

6. COMPARISON OF TENSION SOFTENING CURVES

6.1 Material Properties of Concrete

The compressive strength, tensile strength, and fracture energy of the three types of concrete used in this study are shown in Table 2.

Table 2. Properties of Concrete

age	1 day			3 days			7 days			28 days		
type of concrete	f_c'	f_t	G_F	f_c'	f_t	G_F	f_c'	f_t	G_F	f_c'	f_t	G_F
self-compacting	353	34	0.100	478	45	0.136	538	49	0.146	721	58	0.155
high-strength	597	52	0.114	744	57	0.142	840	58	0.149	966	59	0.157
normal-strength	134	16	0.092	255	28	0.093	291	33	0.101	365	38	0.108

* f_c' : kgf/cm2, f_t : kgf/cm2, G_F : kgf/cm

6.2 Various Evaluation Methods and Tension Softening Curves

In order to confirm the appropriateness of the proposed method, the tension softening curves obtained by various methods are compared. The methods chosen for comparison with our proposed method are the new J-integral method, the modified J-integral method, and the inverse analysis method. Based on the results of this comparison, characteristics, the advantages and disadvantages of the various methods are compared. The estimated value of initial softening stress by all methods does not exactly coincide with the tensile strength of concrete obtained through the splitting test. Therefore,

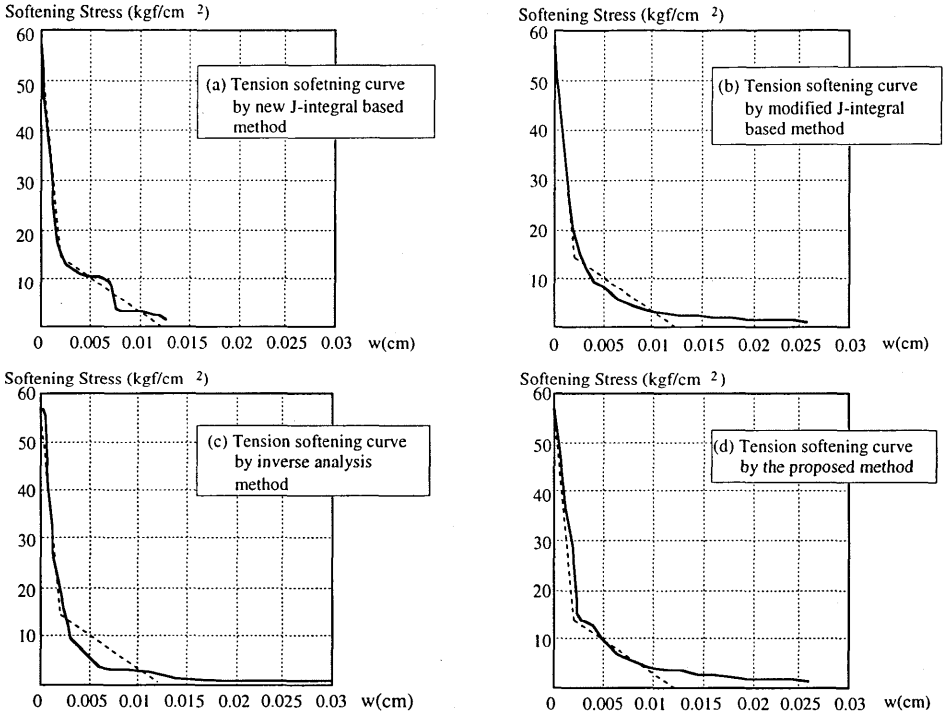

Figure 21. Tension Softening Curves for High-Strength Concrete (Age = 3 Days)

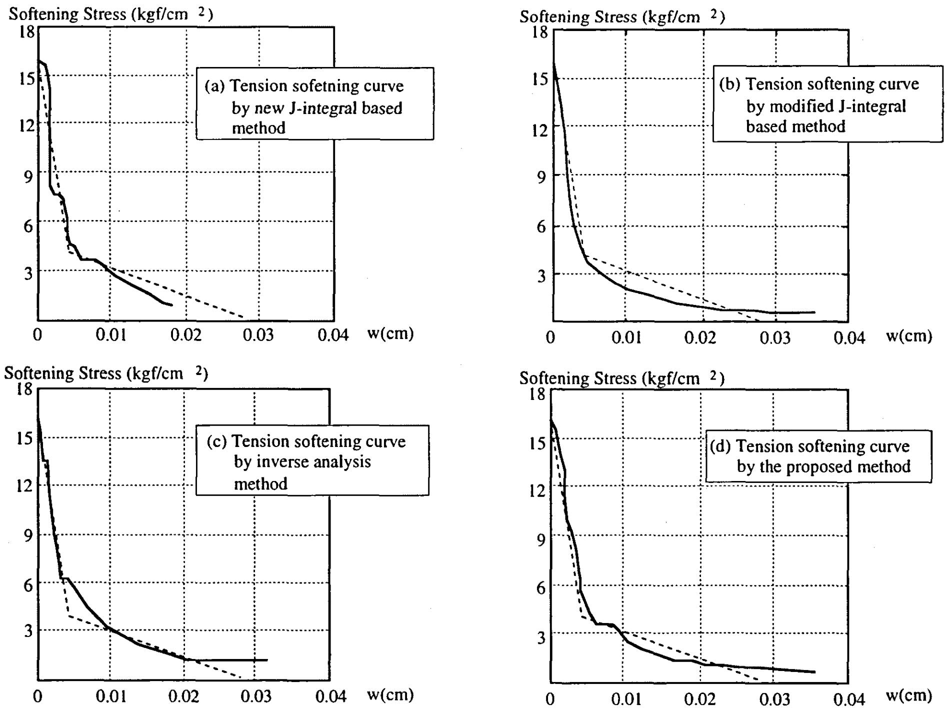

Figure 22. Tension Softening Curves for Normal-Strength Concrete (Age = 1 Day)

the initial softening stress is replaced with the tensile strength of the concrete on the tension softening curve.

Figures 20 to 22 show tension softening curves for self-compacting concrete, high-strength concrete, and normal-strength concrete. In each figure, the tension softening curves estimated by the new J-integral method, the modified J-integral method, the inverse analysis method, and the proposed method are shown; the broken lines represent the 1/4 tension softening model proposed by Rokugo, et al. [7]. For the inverse analysis method, the analysis program [8] proposed by the size effect sub-committee of the concrete committee at JSCE was utilized.

From Figures 20 to 22, the following observations can be noted:

a) The tail portion of the tension softening curve estimated by the new J-integral method is shorter and ends at an earlier stage than curves estimated using other methods. This may be because it is assumed that the ligament portion of the notched beam is subjected to conditions equivalent to uniform tensile force, and the fictitious crack width is one-half of the crack mouth opening.

b) Since the 1/4 model is known for its good conformity with test data, this is considered to be a typical tension softening curve. Tension softening curves obtained from the new J-integral method resemble those of the 1/4 model for each type of concrete. However, there is some oscillation in the curves Therefore, results obtained from the new J-integral method should be used for only rough estimations.

c) Compared with the new J-integral method, tension softening curves obtained from the modified J-integral method were considerably smoother for each type of concrete. Further, a long tail portion, where stress gradually decreases as the fictitious crack width increases, can also be estimated. Therefore, as a method of estimating the tension softening curve, this method seems fairly satisfactory. However, since a close examination of, for instance, a portion of the flat inclination of the tension softening curve (corresponding to the second inclined portion of the 1/4 model), indicates some difference between this method and the 1/4 model, there is some room for improvement.

d) For the inverse analysis method, as described above, the analysis program proposed by the size effect sub-committee of the Concrete Committee at JSCE was used. Further, in this method, the tolerance was fixed at about 0.01. The results obtained by the inverse analysis method were unexpectedly different from those of the 1/4 model. In the inverse analysis method, actual determination of the steep portion of the tension softening curve (corresponding to the first inclined portion of the 1/4 model) should be made at the stage before the fictitious crack propagates significantly. Therefore, the earlier portion of the tension softening curve seems sensitive to the effects of experimental error and tolerance. It seems that the difference in tension softening curves between the 1/4 model and the inverse analysis method is affected by this factor.

e) The tension softening curve obtained from the proposed method, in which the modified J-integral method is further modified in the two areas described, is slightly lacking in smoothness when compared to that obtained by the modified J-integral method, but the deviation in the flat portion when compared with the 1/4 model is considerably improved. In addition, the long tail portion of the tension softening curve can also be estimated. With the proposed method, it may be possible to estimate a tension softening curve resembling that of the 1/4 model regardless of the type of concrete.

6.3 Main Factors Affecting the Proposed Method

In the proposed method, the modified J-integral method is further improved by (1) deducting the released portion of elastic energy, and (2) evaluating the fictitious crack propagation. An examination was carried out to determine which of the above two modifications has a greater effect on the results obtained using the proposed method.

Figure 23 shows results of estimating the tension softening curves for self-compacting concrete by (a) the modified J-integral method, (b) the modified J-integral method and release of elastic energy, (c) the modified J-integral method and fictitious crack propagation, and (d) the proposed method.

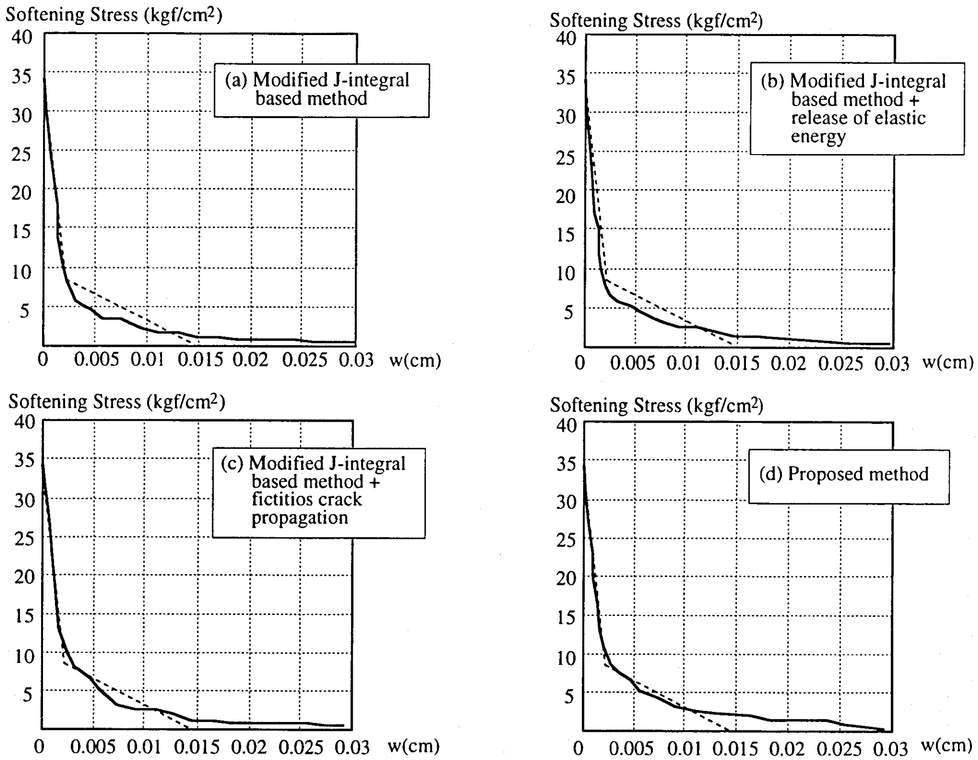

Figure 23. Main Factors Affecting the Proposed Method (Self-Compacting Concrete at 1 Day)

In the case of (b), in which the release of elastic energy is taken into account, the tension softening curve obtained more closely resembles the 1/4 model, in comparison with (a), so consideration of the release of elastic energy contributes to improved accuracy of the tension softening curve.

In the case of (c), where fictitious crack propagation is considered, the tension softening curve also resembles the 1/4 model more closely than in (a), where only the modified J-integral method is adopted. Further, in both the steep portion immediately after softening and the flat portion that follows, case (c) more closely resembles the 1/4 model than case (b). This suggests that appropriate evaluation of fictitious crack propagation is more important than the release of elastic energy.

As Figure 23(d) shows, the proposed method, in which both of these two corrections are taken into consideration, the deviation from the 1/4 model is small in comparison to the modified J-integral method, and the estimated long tail portion qualitatively coincides with the softening behavior of actual concrete. However, judging from the results shown in Figure 23(b) and (c), it seems more important to model the fictitious crack propagation than the release of elastic energy.

7. CONCLUSIONS

In this paper, an experimental method of determining the tension softening curve of concrete based on the energy balance concept and using a J-integral method is studied. The conventional modified J-integral method was further modified by estimating the release of elastic energy and fictitious crack propagation in the ligament portion of a beam. The elastic energy was taken into account by implementing repeated unloading and reloading tests in the softening region, and the residual deflection was quantitatively evaluated at maximum deflection and at unloading. Further, fictitious crack propagation was quantitatively evaluated based on measured data obtained using π-type displacement gages fitted to the ligament portion. The following conclusions were reached through this study:

1) The tension softening curve obtained with the proposed method, in which two shortcomings of the modified J-integral method were further modified, is somewhat lacking in smoothness when compared to that obtained with the modified J-integral method, but is superior to that obtained with the modified J-integral method in its conformity to the 1/4 model, which is considered the standard tension softening curve of concrete.

2) The tension softening curve obtained using the inverse analysis method was, surprisingly, quite different from that of the 1/4 model; however, the first half of the steep portion of the tension softening curve should be determined before the fictitious crack has propagated very much. It therefore seems that this method would be sensitive to experimental errors and other factors.

3) Of the two modifications adopted for the proposed method, the evaluation of fictitious crack propagation was recognized as being more important than the release of elastic energy.

References

[1] Kitsutaka, Y., Kamimura, K., Nakamura, S., "Polylinear Approximation Analysis of Tension Softening Diagram for Concrete", Journal of Structural and Construction Engineering, Architectural Institute of Japan, No. 453, pp. 15-25, 1993 (in Japanese).
[2] Kurihara, N., Ando, T., Kunieda, M., Uchida, Y., Rokugo, K., "Determination of Tension Softening Diagram of Concrete by Poly-Linear Approximation Analysis and Flexural Failure Behavior of Fiber Reinforced Concrete", Journal of Materials, Concrete Structures and Pavements of JSCE, No. 532, V-30, pp. 119-129, 1996 (in Japanese).
[3] Kitsutaka, Y., Kurihara, N., Mihashi, H., Nakamura, S., "Discussion on Standard Test Methods to Determine Tension Softening Diagram of Cementitious Composites", Proceedings of the Japan Concrete Institute, Vol. 19, No. 2, pp. 27-32, 1997 (in Japanese).
[4] Li, V.C., Ward, R.J., "A Novel Testing Technique for Post-Peak Tensile Behavior of Cementitious Materials", *Fracture Toughness and Fracture Energy*, Balkema, pp. 183-195, 1989.
[5] Rokugo, K, Iwasa, M., Seko, S., Koyanagi, W., "Quantitative Evaluation of Tension Softening Curve of Concrete using J-Integral Method", Proceedings of Cement and Concrete, No. 43, pp. 304-309, 1989 (in Japanese).
[6] Uchida, Y., Rokugo, K., Koyanagi, W., "Estimation and Measurement of Tension Softening Curve Based on Bending Tests", Journal of Materials, Concrete Structures and Pavement of JSCE, No. 426, V-14, pp. 203-212, 1991 (in Japanese).
[7] Rokugo, K., Iwasa, M., Suzuki, T., Koyanagi, W., "Testing Method to Determine Tensile Strain Softening Curve and Fracture Energy of Concrete", *Fracture Toughness and Fracture Energy*, Balkema, pp. 153-163, 1989.
[8] Size Effect Sub-Committee of the Concrete Committee at JSCE, "Size Effect in Structural Concrete and Tension Softening Curves of Concrete", *Concrete Technology Series*, No. 18, 92 pp., 1997 (in Japanese).